

CONSTITUTIVE MODELLING OF FIBRE-REINFORCED CONCRETE UNDER UNIAXIAL TENSILE LOADING

Jyrki Kullaa
Technical Research Centre of Finland
Laboratory of Structural Engineering
Kemistintie 3
SF-02150 ESPOO
FINLAND

Rakenteiden Mekaniikka, Vol. 25
No 4 1992, ss. 24 - 49

ABSTRACT

The mechanics of fibre-reinforced concrete under uniaxial loading is studied. The main part of the study considers the behaviour after cracking.

A new constitutive model is developed. It takes into account the strain-softening part of the stress-strain curve. In addition, the crack distance and crack width are calculated. The fibres are smooth and straight. They can be short or continuous, aligned or randomly distributed, brittle or ductile, hard or soft. Moreover, different types of fibres may lie in the same matrix. The model takes into account single-fracture or multicracking states and different fracture mechanisms: fibre fracture or pull-out.

The results of the new model are promising. The effects of different parameters can be studied and even new formulas can be found. The model can also be used in the design of composite materials.

INTRODUCTION

Fibre reinforcement has been shown to improve the tensile behaviour of concrete. With just a few percent of fibres the toughness increases, and with a larger amount of fibres the tensile strength also increases.

In FRC composites, the major effect of the fibres is noted in the post-cracking case, where the fibres bridge across the cracked matrix (Bentur & Mindess 1990).

The composite may fail in a single-fracture mode or if the fibre volume content is high, it is possible to reach the multiple-cracking stage of the matrix.

In the single-fracture mode the bridging of fibres across the crack to transfer the load is usually simulated by pull-out tests, but in the multiple cracking mode the simulation is no longer possible. In pulling a fibre from a cracked matrix the load carried by the fibre in every crack must be equal to the external force (Fig. 1).

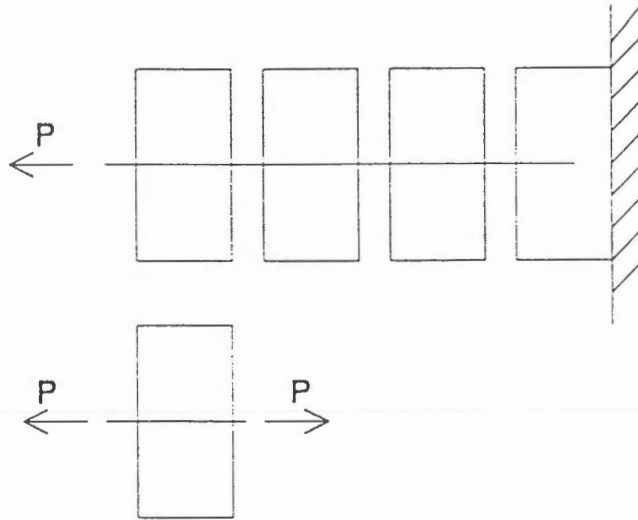


Figure 1. Pull-out of the fibre from the cracked matrix and a free body diagram of the composite between two cracks.

Wang (1985) developed a theoretical statistical model to predict the stress-strain curve of fibre-reinforced concrete in the single-fracture mode. The bond was assumed to be constant frictional. The fibres are in a 3-dimensional random distribution.

The ACK model predicts the stress-strain behaviour in the multiple and post-multiple cracking stages. The model takes into account the fibre length and orientation by efficiency factors. The strain softening region is not included in the ACK model.

A NEW CONSTITUTIVE MODEL

The new proposed model takes into account the single-fracture or multiple-cracking states and different fracture mechanisms: fibre fracture or pull-out. The fibres may be short or continuous, aligned or randomly distributed, brittle or ductile, hard or soft. Moreover, different types of fibres may lie in the same matrix (hybrid fibre composite). The fibres are supposed to carry only axial tensile stress. The bending effect and the concentrated friction force at the fibre exit point are neglected. The fibres are assumed to be independent. The fibre breakage and sliding are taken into account.

The constitutive model is strain-controlled: The strain is increased monotonically and the corresponding composite stress is evaluated. Thus also the

strain-softening part of the stress-strain curve can be taken into account.

The crack is assumed to initiate when the matrix stress or strain reaches the critical value, σ_{mu} or ϵ_{mu} , respectively. In the multiple-cracking state the initial crack distance is chosen to be half of the length of the longest fibre type. At more advanced stages of loading, new cracks are assumed to initiate between the already-existing cracks so that the crack distances are equal. The crack widths are supposed to be equal.

Assuming that the fibres are independent, the contribution of the fibres may be superposed. For example, in hybrid reinforcement different types of fibres can be analyzed separately or fibres with different embedded lengths may be averaged.

The stress of the composite can be evaluated by dividing the sum of the forces carried by the fibres bridging the crack by the area of the composite cross-section.

$$\begin{aligned}
 \sigma_c &= \frac{F_c}{A_c} \\
 &= \frac{1}{A_c} \sum_{i=1}^N P_i \\
 &= \frac{1}{A_c} (N_1 \bar{P}_1 + N_2 \bar{P}_2 + \dots + N_n \bar{P}_n) \\
 &= \frac{V_{f1} \bar{P}_1}{A_{f1}} + \frac{V_{f2} \bar{P}_2}{A_{f2}} + \dots + \frac{V_{fn} \bar{P}_n}{A_{fn}} \\
 &= \sum_{j=1}^n V_{fj} \bar{\sigma}_{fj}
 \end{aligned} \tag{1}$$

where F_c is the external tensile force, A_c is the area of the composite cross-section, P_i is the force carried by a fibre, A_{fi} is the area of the cross-section of one fibre type, N is the number of fibres bridging the crack, N_i is the number of fibres of one type bridging the crack, n is the number of different fibre types, V_{fi} is the fibre volume content of one fibre type and \bar{P}_i and $\bar{\sigma}_{fj}$ are the average force and the average stress, respectively, carried by a fibre of one type.

UNCRACKED COMPOSITE

Before cracking, the behaviour is assumed to follow the rules of mixtures:

$$\sigma_c = (E_m V_m + \sum \eta_i \eta_\theta E_f V_f) \epsilon_c \tag{2}$$

where ϵ_c is the strain of the composite, E_m and E_f are the moduli of elasticity of the matrix and the fibre, respectively, V_m and V_f ($V_m = 1 - \sum V_f$) are the volume contents of the matrix and the fibre, respectively, and η_l and η_θ are the efficiency factors of fibre length and orientation, respectively.

The first crack is initiated when the composite strain reaches the critical value, ϵ_{cu} .

SINGLE FRACTURE

After the first crack, the situation in the vicinity of the crack can be modelled by the pull-out of fibres of different lengths and orientations simultaneously. The uncracked composite is modelled by the rules of mixtures.

The stress of the composite is

$$\sigma_c = \sum V_f \overline{\sigma_f(l, \theta)} \quad (3)$$

where l is the fibre embedded length and θ is the fibre orientation angle.

The average fibre stress is obtained as follows. Let l_f be the length of the fibre. After Wang & al (1989) fibres whose centroids are located at a distance of $l_f/2$ or less from the crack plane may intercept the crack plane. The distance of the fibre centroid from the crack plane for these fibres is uniformly distributed from 0 to $l_f/2$, with a constant probabilistic density function

$$p(z) = \frac{2}{l_f} \quad 0 \leq z \leq l_f/2 \quad (4)$$

A fibre whose centroid is at a distance z from the crack plane will intercept the crack if

$$\frac{l_f}{2} \cos \theta \geq z \quad (5)$$

Let us assume that the fibres are randomly oriented over the angle interval from θ_1 to θ_2 measured from the direction of the external load. Thus, the probability of a fibre intercepting the crack plane can be evaluated from

$$\int_{\theta_1}^{\theta_2} \left[\int_{z=0}^{\frac{l_f}{2} \cos \theta} p(z) dz \right] p(\theta) d\theta = \int_{\theta_1}^{\theta_2} p(\theta) \cos \theta d\theta \quad (6)$$

where $p(\theta)$ is the probabilistic density function of the distribution of the fibre orientation. In a 3-dimensional distribution $p(\theta)$ is

$$p(\theta) = \frac{1}{A} \frac{dA}{d\theta} = \frac{2\pi l^2 \sin \theta}{2\pi l^2 (\cos \theta_1 - \cos \theta_2)} = \frac{\sin \theta}{\cos \theta_1 - \cos \theta_2} \quad (7)$$

and in a 2-dimensional distribution

$$p(\theta) = \frac{1}{s} \frac{ds}{d\theta} = \frac{l}{l(\theta_2 - \theta_1)} = \frac{1}{\theta_2 - \theta_1} \quad (8)$$

A is the area of the spherical surface and s is the arc-length.

The average stress in the fibre can be evaluated from

$$\bar{\sigma}_f = \frac{1}{C} \frac{2}{l_f} \int_0^{l_f/2} \left[\int_C \sigma_f(l, \theta) \cos \theta dC \right] dl \quad (9)$$

where C represents either A or s . For a 3-dimensional distribution, the average stress is

$$\bar{\sigma}_f = \frac{2}{l_f} \frac{1}{\cos \theta_1 - \cos \theta_2} \int_0^{l_f/2} \left[\int_{\theta_1}^{\theta_2} \sigma_f(l, \theta) \sin \theta \cos \theta d\theta \right] dl \quad (10)$$

and for a 2-dimensional distribution

$$\bar{\sigma}_f = \frac{2}{l_f} \frac{1}{\theta_2 - \theta_1} \int_0^{l_f/2} \left[\int_{\theta_1}^{\theta_2} \sigma_f(l, \theta) \cos \theta d\theta \right] dl \quad (11)$$

In single-fracture mode, the fibre stress does not depend on the fibre orientation. Therefore one can use the orientation efficiency factor η_θ , as will be shown.

The average fibre stress can now be evaluated from

$$\bar{\sigma}_f = \frac{1}{C} \frac{2}{l_f} \int_0^{l_f/2} \sigma_f(l) \left[\int_C \cos \theta dC \right] dl \quad (12)$$

which for a 3-dimensional distribution is

$$\begin{aligned}
\overline{\sigma}_f &= \frac{2}{l_f} \frac{1}{\cos \theta_1 - \cos \theta_2} \int_0^{l_f/2} \sigma_f(l) \left[\int_{\theta_1}^{\theta_2} \sin \theta \cos \theta d\theta \right] dl \\
&= \frac{\sin^2 \theta_2 - \sin^2 \theta_1}{2(\cos \theta_1 - \cos \theta_2)} \frac{2}{l_f} \int_0^{l_f/2} \sigma_f(l) dl \\
&= \eta_\theta \frac{2}{l_f} \int_0^{l_f/2} \sigma_f(l) dl
\end{aligned} \tag{13}$$

where

$$\eta_\theta = \frac{\sin^2 \theta_2 - \sin^2 \theta_1}{2(\cos \theta_1 - \cos \theta_2)} \tag{14}$$

For a 2-dimensional distribution

$$\begin{aligned}
\overline{\sigma}_f &= \frac{2}{l_f} \frac{1}{\theta_2 - \theta_1} \int_0^{l_f/2} \left[\int_{\theta_1}^{\theta_2} \sigma_f(l) \cos \theta d\theta \right] dl \\
&= \frac{\sin \theta_2 - \sin \theta_1}{\theta_2 - \theta_1} \frac{2}{l_f} \int_0^{l_f/2} \sigma_f(l) dl \\
&= \eta_\theta \frac{2}{l_f} \int_0^{l_f/2} \sigma_f(l) dl
\end{aligned} \tag{15}$$

where

$$\eta_\theta = \frac{\sin \theta_2 - \sin \theta_1}{\theta_2 - \theta_1} \tag{16}$$

One can notice that for randomly distributed fibres ($\theta_1 = 0, \theta_2 = \pi/2$), the probabilities in 3- and 2-dimensional distributions are $1/2$ and $2/\pi$, respectively. Moreover, according to L'Hôpital's rule the probability of aligned fibres is $\cos \theta$ in both cases.

In the multicracking state, the orientation efficiency factors obtained above can no longer be used, while the fibre stress depends also on the orientation of the fibres. Then the general Equation 9 should be used.

The stress and strain of the composite are

$$\sigma_c = \sum \eta_\theta V_f \frac{\overline{P}}{A_f} \tag{17}$$

$$\epsilon_c = \frac{\sigma_c}{V_m E_m} + \frac{w}{L} \tag{18}$$

where L is the length of the test specimen, w is the crack width which can be calculated by summing the displacements of the fibre on both sides of the crack.

$$w = \Delta_1 + \Delta_2 \quad (19)$$

$$\Delta_1 = \Delta_1(P, l) \quad (20)$$

$$\Delta_2 = \Delta_2(P, l_f - l) \quad (21)$$

Δ_1 ja Δ_2 are the displacements of the shorter and longer embedded lengths of the fibre, respectively. l is the shorter embedded length and l_f is the length of the fibre. The relation $\Delta_1(P, l)$ can be obtained by pull-out tests of different embedded fibre lengths, or by one pull-out test from which the bond parameters are obtained and using a theory in deriving the pull-out curves for different embedded fibre lengths. In this study the theory of Naaman & al. (1991) is used.

The shorter embedded length l is uniformly distributed from 0 to $l_f/2$. At a fibre displacement Δ_1 , the average force carried by a fibre is calculated by

$$\bar{P} = \frac{2}{l_f} \int_0^{l_f/2} P(l, \Delta_1) dl \quad (22)$$

MULTIPLE CRACKING

If the fibre content is sufficiently high, it is possible that the load-bearing capacity of the fibres is greater than the load on the composite at the first crack. Additional loading will result in additional cracks, until the matrix is divided into a number of segments, separated by cracks. The cracking stops when the stress transferred to the matrix no longer exceeds the cracking stress.

For simplicity, constant frictional stress transfer between fibres and matrix is assumed. It is also assumed that the crack spacings of different cracks are equal and that the crack widths of different cracks are equal.

When the normal force of the fibre in the crack is P , the fibre displacement in the crack can be evaluated as follows. The local tensile force F in the fibre is

$$F(x) = P - t_f x \quad (23)$$

where t_f is the shear flow at the fibre-matrix interface. It is the product of the shear stress and the perimeter of the fibre: $t_f = \tau_f \psi$. x is the distance from the crack.

Let us assume that the matrix carries the transferred force with the area A_m . The strain difference between the fibre and the matrix is

$$\epsilon_f - \epsilon_m = \frac{F(x)}{A_f E_f} - \frac{P - F(x)}{A_m E_m} = \frac{P - t_f x}{A_f E_f} - \frac{t_f x}{A_m E_m} \quad (24)$$

The displacement of the fibre in the crack is evaluated by

$$\Delta = \int_0^c (\epsilon_f - \epsilon_m) dx = \frac{Pc}{A_f E_f} - \frac{1}{2} t_f c^2 \left(\frac{1}{A_m E_m} + \frac{1}{A_f E_f} \right) \quad (25)$$

where c is the distance from the crack where the fibre carries tension.

Fibres whose shorter embedded length is less than $l_x/2$ will slip. In constant frictional stress transfer, it can be calculated from

$$\frac{l_x}{2} = \frac{P}{t_f} \quad (26)$$

Substituting $c = P/t_f$ in Equation 25, solving P/t_f and taking the Equation 26 into account, leads to

$$\frac{l_x}{2} = \sqrt{\frac{2\Delta}{t_f} \left(\frac{1}{A_f E_f} - \frac{1}{A_m E_m} \right)^{-1}} \quad (27)$$

Let l be the embedded fibre length. At first, it is assumed that the fibres are aligned. Futhermore it is assumed that there exists a symmetrical fibre in the neighbouring crack with respect to the fibre being studied (see Figures 2-7). The crack spacing is $2s$. In Figures 2-7 on the left-hand side the tensile forces in the fibre and in the symmetry fibre between two cracks are showed. The end of the line represents the fibre end. On the right-hand side the normal forces of the two fibres between the cracks are superposed to produce simpler formulas. The arrow represents the fibre force acting in the crack.

There are a few different force-transferring cases:

1. If $l \leq l_x/2$, the fibre slips and $P = t_d l$, where t_d is the dynamic shear flow.

$$c = l_x/2 \quad (28)$$

$$h_1 = 0 \quad (29)$$

$$h_2 = 0 \quad (30)$$

2. If $l > l_x/2$

$$a = 2s - \frac{1}{2}(l - l_x/2)$$

a is in Figure 7, with c the distance of the intersection point from the crack, as shown.

(a) If $a > l_x/2$, the fibre slips in the neighbouring crack. The force is totally transferred to the matrix (Figures 2, 3 and 4).

$$c = l_x/2 \quad (31)$$

$$h_1 = \min(2s - c, l_x/2) \quad (32)$$

$$h_2 = \min(l - 2s, l_x/2) \quad (33)$$

(b) If $2s - l + l_x/2 < 0$, the fibre does not slip in the neighbouring crack. The forces of the fibre in both cracks are equal (Figures 5 and 6).

$$c = \min(s, l_x/2) \quad (34)$$

$$h_1 = h_2 = c \quad (35)$$

(c) If $a \leq l_x/2$, the fibre slips in the neighbouring crack. The force is partially transferred to the matrix (Figure 7).

$$c = a \quad (36)$$

$$h_1 = h_2 = 2s - c \quad (37)$$

where h_1 and h_2 are the distances from the crack where the superposed forces change to be constant. The values are needed in calculating the stress and strain of the matrix.

The force carried by the fibre in the crack can be solved from Equation 25:

$$P = \frac{A_f E_f}{c} \Delta + \frac{1}{2} t_f c \left(1 + \frac{A_f E_f}{A_m E_m} \right) \quad (38)$$

The crack width is found by summing the fibre displacements of both embedded lengths.

In the cases 2b (Figure 5) and 2c (Figure 7) an iteration has to be carried out. By substituting P in Equation 26 a new value of the embedded length $l_x/2$ is obtained. After that the force transferring cases are studied, from which a new value of c is obtained. It is substituted in Equation 38. The iteration is repeated until the change of the force P is satisfactorily small.

Because of the new possible crack, the stress or strain in the matrix between the cracks must be studied. In addition, the average strain in the matrix is calculated.

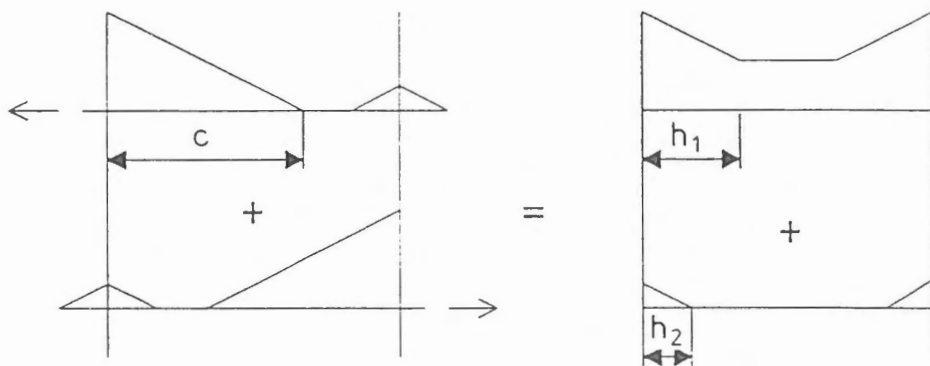


Figure 2. $2s - \frac{1}{2}(l - l_x/2) > l_x/2$. The fibre slips in the neighbouring crack. The force is totally transferred to the matrix. $c = l_x/2$, $h_1 = \min(2s - c, l_x/2) = 2s - c$, $h_2 = \min(l - 2s, l_x/2) = l - 2s$.

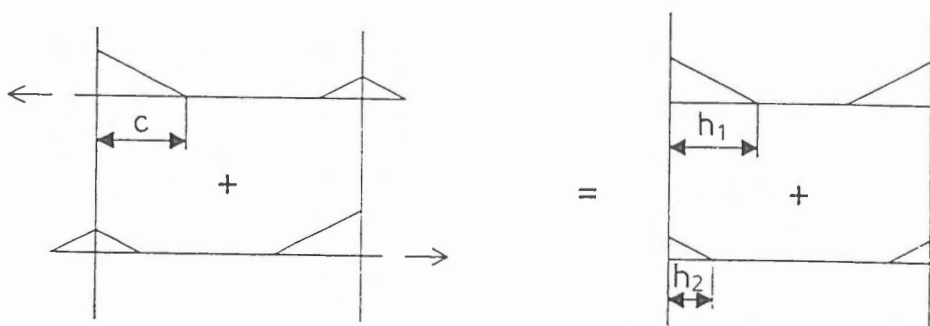


Figure 3. $2s - \frac{1}{2}(l - l_x/2) > l_x/2$. The fibre slips in the neighbouring crack. The force is totally transferred to the matrix. $c = l_x/2$, $h_1 = \min(2s - c, l_x/2) = l_x/2$, $h_2 = \min(l - 2s, l_x/2) = l - 2s$.

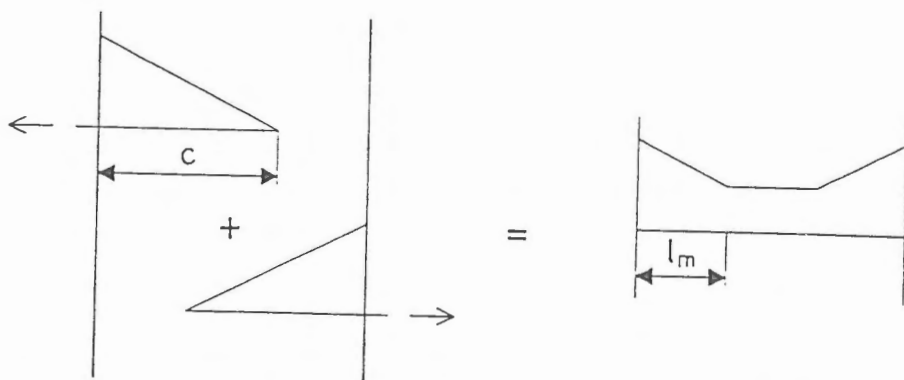


Figure 4. $2s - \frac{1}{2}(l - l_x/2) > l_x/2$. The fibre slips in the neighbouring crack. The force is totally transferred to the matrix. $c = l_x/2$, $l_m = \min(2s - l, l_x/2) = 2s - l$.

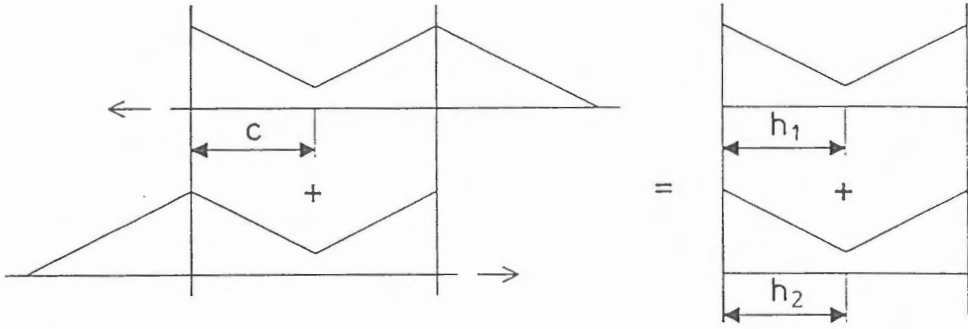


Figure 5. $2s - l + l_x/2 < 0$. The fibre does not slip in the neighbouring crack. The forces of the fibre in both cracks are equal. $c = \min(s, l_x/2) = s$, $h_1 = h_2 = c$.

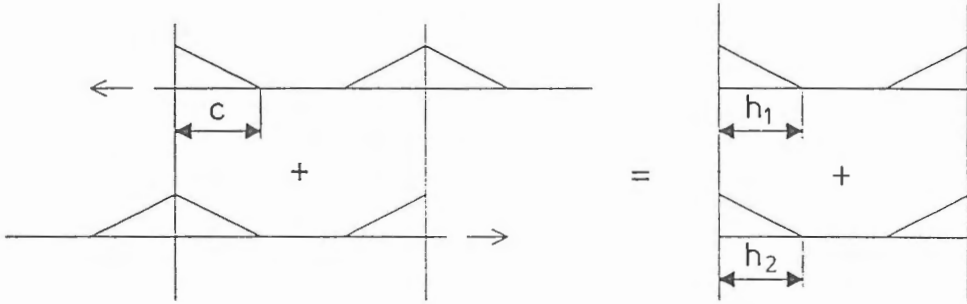


Figure 6. $2s - l + l_x/2 < 0$. The fibre does not slip in the neighbouring crack. The forces of the fibre in both cracks are equal. $c = \min(s, l_x/2) = l_x/2$, $h_1 = h_2 = c$.

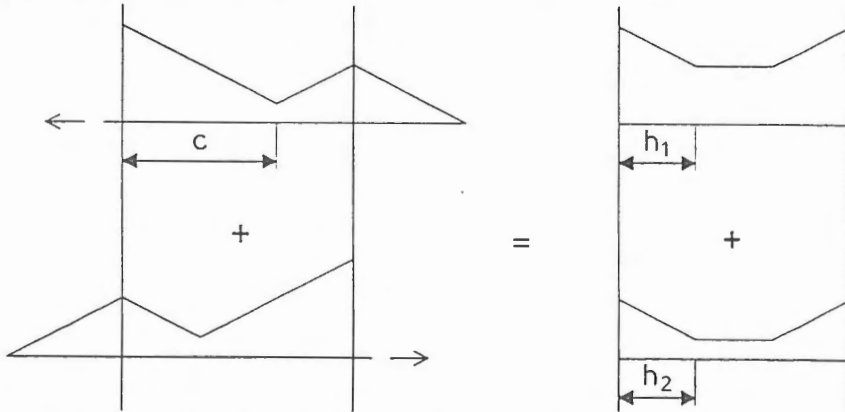


Figure 7. $a = 2s - \frac{1}{2}(l - l_x/2) < l_x/2$. The fibre slips in the neighbouring crack. The force is partially transferred to the matrix. $c = a$, $h_1 = h_2 = 2s - c$.

The strain of the matrix is evaluated by

$$\epsilon_m = \frac{\sigma_m}{E_m} = \frac{T(x)}{A_m E_m} = \frac{P - F(x)}{A_m E_m} \quad (39)$$

where σ_m is the stress of the matrix, and $T(x)$ is the normal force transferred to the matrix. The average force is

$$\overline{T(x)} = \frac{1}{s} \int_0^s T(x) dx \quad (40)$$

If ϵ_m exceeds the cracking strain, a new crack may initiate in the point where the excess occurs. The maximum strain is always in the middle of the matrix between the existing cracks, so the crack spacing is halved.

Let us examine the forces transferred from fibres with different embedded lengths. Figure 8 shows that fibre embedded lengths from 0 to $l_f/2 + s$ must be studied. The longer fibres are symmetry fibres.

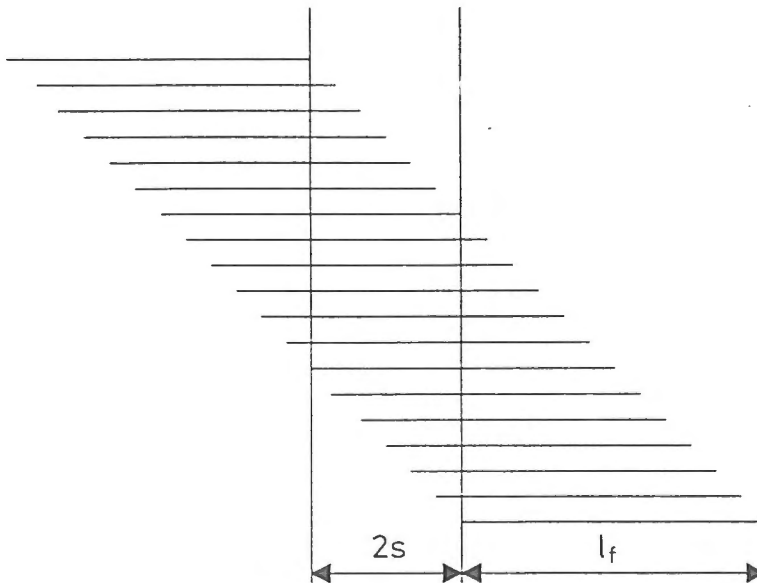


Figure 8. The distribution of fibres between two cracks.

1. $l > 2s$.

The fibre and its symmetry fibre are situated overlapping between the cracks.

$$h_2 \leq h_1.$$

$$T(x) = \begin{cases} 2t_f x, & 0 \leq x \leq h_2 \\ t_f(x + h_2), & h_2 \leq x \leq h_1 \\ t_f(h_1 + h_2), & h_1 \leq x \leq s \end{cases} \quad (41)$$

$$T(s) = \begin{cases} 2t_f s, & h_2 > s \\ t_f(s + h_2), & h_1 > s \\ t_f(h_1 + h_2), & h_1 < s \end{cases} \quad (42)$$

$$\overline{T(x)} = \begin{cases} t_f s, & h_2 > s \\ \frac{1}{s} t_f \left(\frac{1}{2} s^2 - \frac{1}{2} h_2^2 + h_2 s \right), & h_1 > s \\ \frac{1}{s} t_f \left(-\frac{1}{2} h_1^2 - \frac{1}{2} h_2^2 + h_1 s + h_2 s \right), & h_1 < s \end{cases} \quad (43)$$

2. $l < s$ or $s > l_x/2$.

The fibre and its symmetry fibre or their normal forces are not situated overlapping between the cracks.

$$T(x) = \begin{cases} t_f x, & 0 \leq x \leq c \\ P, & c \leq x \leq s \end{cases} \quad (44)$$

$$T(s) = P \quad (45)$$

$$\overline{T(x)} = \frac{1}{s} \left(\frac{1}{2} t_f c^2 + P s - P c \right) \quad (46)$$

3. $s < l_x/2$ and $s < l \leq 2s$.

The fibre and its symmetry fibre and their normal forces are situated partially overlapping between the cracks.

$$l_m = \min(2s - l, l_x/2)$$

$$T(x) = \begin{cases} t_f x, & 0 \leq x \leq l_m \\ t_f l_m, & l_m \leq x \leq s \end{cases} \quad (47)$$

$$T(s) = t_f l_m \quad (48)$$

$$\overline{T(x)} = \frac{1}{s} t_f \left[\frac{1}{2} l_m^2 + l_m (s - l_m) \right] \quad (49)$$

The average force in the middle of the matrix between the cracks is

$$\overline{T(s)} = \frac{1}{l_f} \int_0^{l_f} T(s) dl \quad (50)$$

and the average matrix strain can be evaluated by

$$\overline{\epsilon_m} = \frac{1}{l_f} \frac{1}{A_m E_m} \int_0^{l_f} \overline{T(x)} dl \quad (51)$$

The formulas are also valid for long fibres that extend over several cracks. The stress and strain of the composite can be evaluated by

$$\sigma_c = V_f \frac{\overline{P}}{A_f} \quad (52)$$

$$\epsilon_c = \overline{\epsilon_m} + \frac{w}{2s} \quad (53)$$

where the average stress of the fibre \overline{P}/A_f is calculated by Equation 9.

It should be noted that in the multiple-cracking stage the strain is no longer dependent on the specimen length, as it is in single-fracture mode.

In the Appendix the formulas in the multiple-cracking stage for the composite with oriented fibres are presented.

RESULTS

THE INFLUENCE OF DIFFERENT PARAMETERS

The stress-strain curves of different FRC-materials in tension are evaluated. One parameter is varied at a time. The parameters of the base material are as follows: the fibre volume content $V_f = 0.03$, the length of the fibre $l_f = 30$ mm, the fibre diameter $d = 0.5$ mm, the specimen width $L = 50$ mm, the modulus of elasticity of the matrix $E_m = 21$ GPa, the matrix cracking stress $\sigma_{mu} = 3$ MPa, the modulus of elasticity of the fibre $E_f = 207$ GPa, the ultimate strength of the fibre $\sigma_{fu} = 1$ GPa and the coefficient of friction $\mu = 0.6$. The following parameters are for modelling the fibre pull-out (see Naaman & al. 1991). The Poisson ratio of the matrix $\nu_m = 0.35$, the Poisson ratio of the fibre $\nu_f = 0.3$, the bond modulus $\kappa = 10^{13}$ N/m³, the bond strength $\tau_{max} = 2.8$ MPa, the frictional bond shear stress $\tau_f = 2.5$ MPa, and the constants in modelling the decreasing friction $\xi = -0.01$ and $\eta = 0.2$. The fibres are

3-dimensionally randomly distributed. The fibres are assumed to break when the stress in a fibre exceeds σ_{fu} .

The diameter of the fibre d is varied from 0.05 mm to infinity and the length of the fibre l_f is varied from 0 to 300 mm, so that the influence of the aspect ratio l_f/d can also be studied. The calculations show that it makes no difference if the fibre length is increased or the fibre diameter is decreased. Figure 9 shows the effect of the aspect ratio on the stress-strain curve. It is seen that increasing the fibre length or decreasing the fibre diameter leads to the strength and toughness increasing until the fibres are so long or thin that they break.

The calculations are strain controlled, i.e. the strain of the composite is increased monotonically. Hence there are jumps in the multiple-cracking stage when new cracks are formed. The sharply descending curve with jumps represents the breaking of fibres.

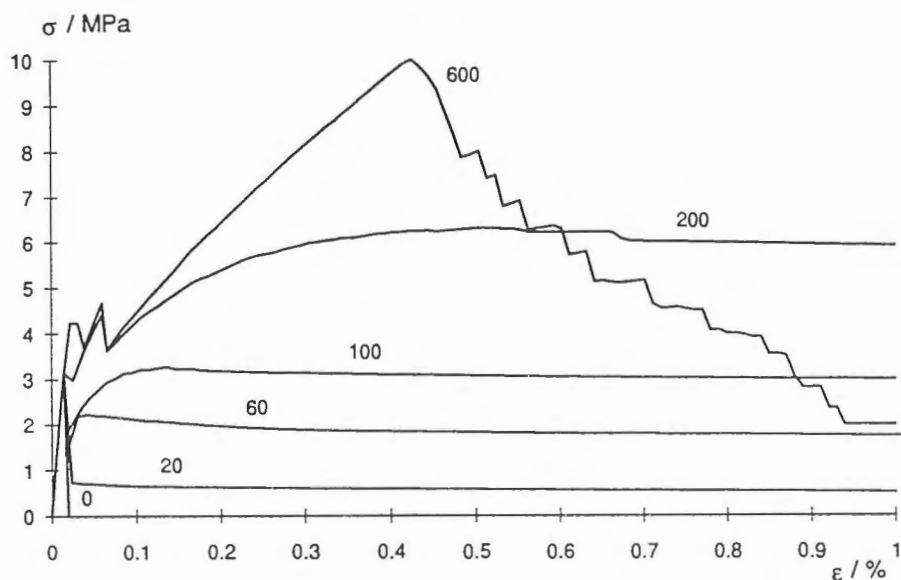


Figure 9. The effect of fibre aspect ratio on the constitutive relation.

In Figure 10 the effect of fibre content is shown. The fibre volume content of the present material must exceed 5 percent for strengthening the composite.

The effect of nylon fibres on steel-fibre-reinforced concrete is studied. The following properties according to Wang & al. (1989) are used. $d = 0.0176$ mm, $l_f = 38.1$ mm, $E_f = 5$ GPa, $\sigma_{fu} = 1$ GPa, $\tau = 0.16$ MPa. The elastic and frictional shear stresses are assumed to be equal, and the other pull-out parameters ν_f , μ , κ , ξ and η are chosen to be the same as for steel fibres.

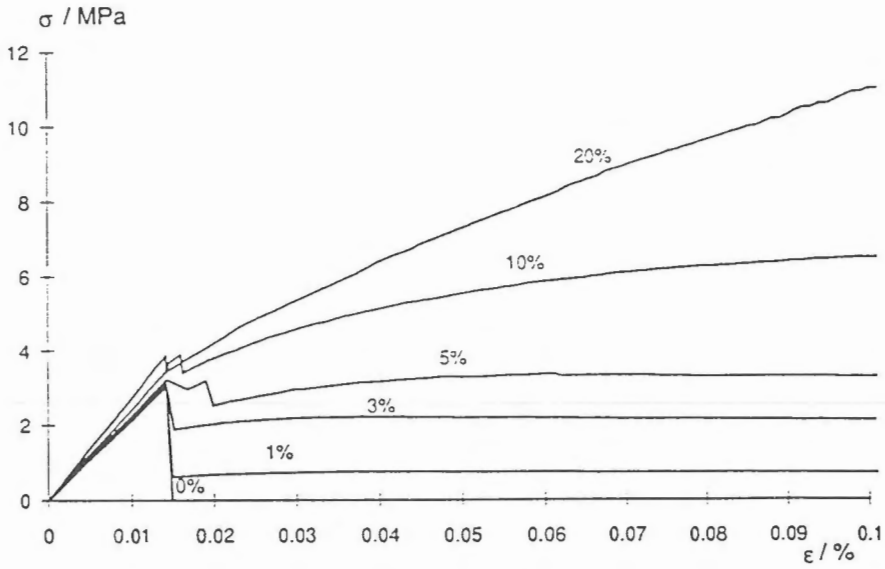


Figure 10. The effect of fibre volume content on the constitutive relation.

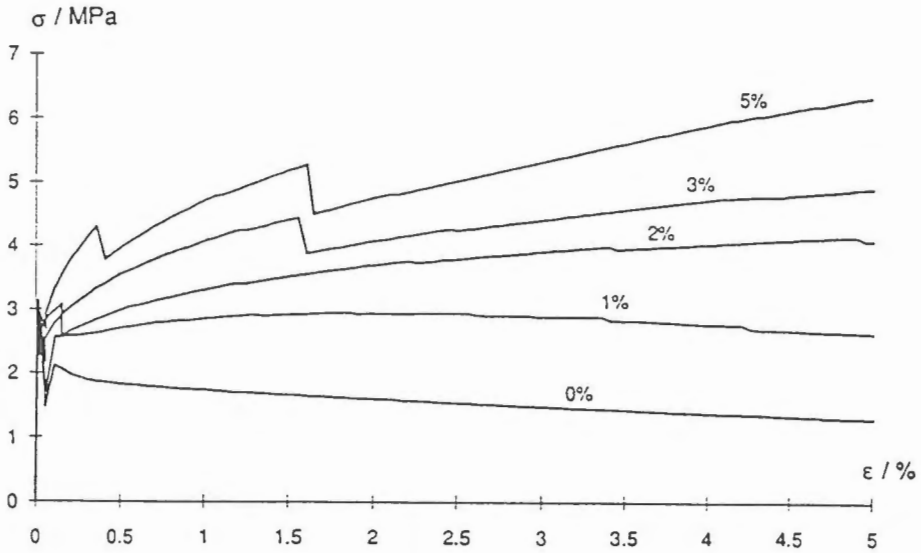


Figure 11. The effect of nylon fibres on the constitutive relation of steel-fibre-reinforced concrete.

From Figure 11 it is seen that by increasing the nylon fibres, the strength of the composite increases. More distinctly, the strain capacity and the toughness increase.

COMPARISON OF THE MODEL WITH THE ACK MODEL

The base material of the previous section is chosen. If the fibres slip, the tensile strength of the composite according to the ACK model is

$$\sigma_{cu} = \eta_0 V_f \tau_f \frac{l_f}{d} \quad (54)$$

where d is the fibre diameter.

The fibre efficiency factor for randomly oriented fibres is $\eta_0 = 0.5$. In Table 1 a comparison of the present and the ACK model is presented.

In Table 1 the mark (B) after the strength value means that a part of the fibres break instead of sliding. It can be seen that the present model gives lower values for the composite strength than the ACK model. Moreover, with a higher strength the relative difference is larger.

When the fracture mode is the fibre breakage, the strength of the composite and the crack distance are examined. According to the ACK model (Aveston & al. 1974) the minimum crack distance for a composite with short, aligned fibres is

$$x_d = \frac{l_f - \sqrt{l_f^2 - 4l_f x}}{2} \quad (55)$$

where x is the minimum crack distance for continuous fibres:

$$x = \frac{V_m \sigma_{mu} d}{V_f 4\tau_f} \quad (56)$$

σ_{mu} is the matrix cracking stress. The crack distance is between x_d and $2x_d$.

The strength of the composite is evaluated by

$$\sigma_{cu} = \left(1 - \frac{l_c}{l_f}\right) \sigma_{fu} V_f \quad (57)$$

where

Table 1. Comparison of the tensile strength between the ACK model and the new model when the fracture mode is fibre sliding. The mark (B) after the strength value means that a part of the fibres break instead of sliding.

d / mm		ACK model $\eta_{\theta} V_f \tau_f l_f / d / \text{MPa}$	New model σ_{cu} / MPa	Relative diff. / %
∞		0	0	0
1.5		0.75	0.75	0
0.5		2.25	2.22	-1.33
0.3		3.75	3.30	-12.0
0.15		7.50	6.47 (B)	-13.7
0.05		22.5	10.1 (B)	-55.1
$V_f / \%$				
0		0	0	0
1		0.75	0.74	-1.33
3		2.25	2.22	-1.33
5		3.75	3.36	-10.4
10		7.5	6.63	-11.6
20		15	13.6	-9.33
τ_f / MPa				
0		0	0	0
2		1.80	1.77	-1.67
4		3.60	3.18	-11.7
6		5.40	4.73	-12.4
8		7.20	6.21	-13.8
12		10.8	8.11 (B)	-24.9
θ	η_{θ}			
0	1	4.5	4.13	-8.22
30	0.866	3.90	3.59	-7.95
60	0.5	2.25	2.22	-1.33
90	0	0	0	0
2-D				
0-30	0.955	4.3	3.95	-8.14
0-60	0.827	3.7	3.42	-7.57
0-90	0.637	2.9	2.82	-2.76
3-D				
0-30	0.933	4.2	3.85	-8.33
0-60	0.75	3.38	3.23	-4.44
0-90	0.5	2.25	2.22	-1.33

$$l_c = \frac{\sigma_{fu}d}{4\tau_f} \quad (58)$$

σ_{fu} is the strength of the fibre.

In calculation, the same base material as in the previous section is used. In Table 2, the material parameters varied are shown. The last two columns show the crack distance and the strength, respectively, according to the proposed model.

Table 2. The crack spacings and the tensile stresses for different FRC composites with short, aligned fibres according to the present model.

l_f mm	V_f %	σ_{fu} MPa	d mm	τ MPa	σ_{mu} MPa	$2s$ mm	σ_{cu} MPa
10	3	400	0.1	2.5	3	1.25	7.31
10	2	400	0.1	2.5	3	2.5	4.30
10	1.5	400	0.1	2.5	3	5.0	3.22
20	1.5	400	0.1	2.5	3	5.0	4.45
20	1.5	400	0.1	2.5	4	5.0	4.45
15	1.5	400	0.1	2.5	4	3.98	3.77
30	3	400	0.1	2.5	4	1.88	10.3
30	3	400	0.1	3.5	4	1.88	10.5
10	5	400	0.1	3.5	4	1.25	13.9
100	2	400	0.1	3.5	4	1.56	7.41
100	2	400	0.5	3.5	4	12.5	6.49
50	2	400	0.5	3.5	4	12.5	4.00
35	2	400	0.5	3.5	4	17.5	4.08
35	2	800	0.2	3.5	4	4.37	10.2
100	2	800	0.2	3.5	4	3.13	13.9

In Figure 12 the crack distances are shown so that the abscissa presents the values obtained by Equation 55 and the ordinate shows the crack distance of the proposed model. In addition, the limits of the crack spacing, $x_d \leq 2s \leq 2x_d$ are presented.

In Figure 13 the composite strength from the new model is presented using the function of Equation 57. In addition, a line with slope 1 has been drawn.

It can be seen that the present model is in a good agreement with the ACK model for composites with short, aligned fibres.

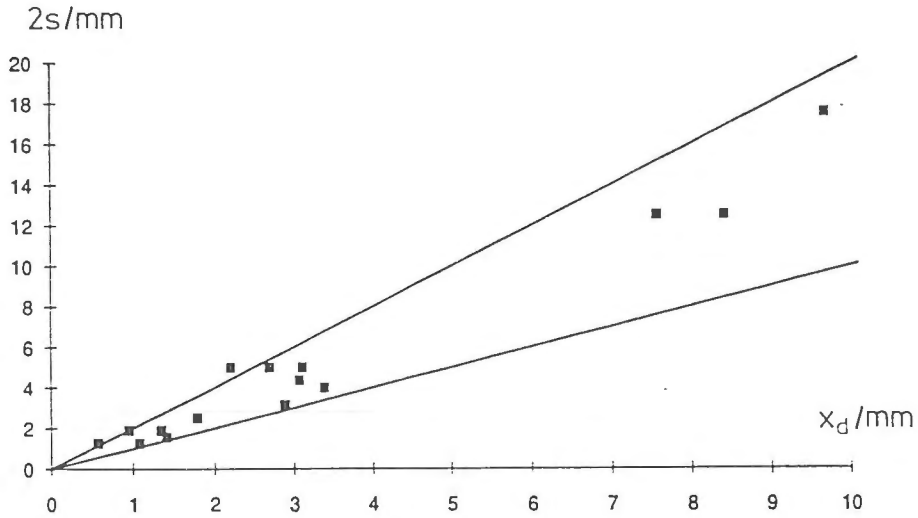


Figure 12. The relationship between the crack spacing of composites with aligned, short fibres according to the present model and according to the ACK model. The lines represent the minimum and maximum crack spacings according to the ACK model.

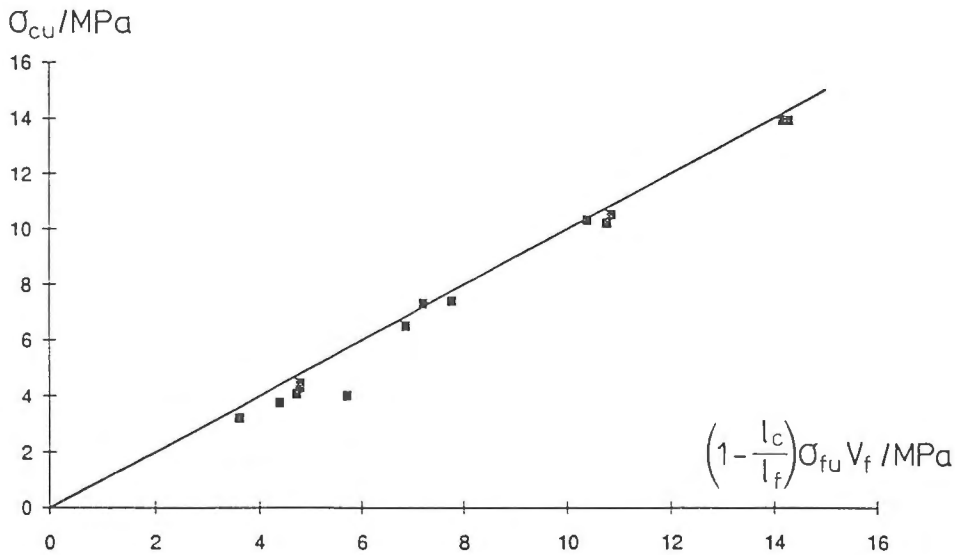


Figure 13. The relationship between the tensile strength of the composite with aligned, short fibres according to the present model and the ACK model.

The crack spacing and the composite strength are calculated also for composites with randomly oriented short fibres. The results are compared to the equations presented above to check if there is a relationship between the present model and the calculated values for short, aligned fibres.

New values for fibre moduli and the tensile strength of the matrix are chosen ($E_f = 5$ GPa, $\sigma_{mu} = 1$ MPa) to make the multicracking possible. In Table 3 the varied parameters, the crack spacing and the tensile strength of the composites are presented.

Table 3. The crack spacings and tensile strengths of different composites with randomly oriented short fibres according to the present model.

l_f mm	V_f %	σ_{fu} MPa	d mm	τ MPa	$2s$ mm	σ_{cu} MPa
10	3	400	0.1	2.5	1.25	2.93
10	2	400	0.1	2.5	2.5	2.01
10	1.5	400	0.1	2.5	5.0	1.55
20	1.5	400	0.1	2.5	2.5	1.95
15	1.5	400	0.1	2.5	3.75	1.86
30	3	400	0.1	2.5	0.938	3.9
30	3	400	0.1	3.5	0.938	4.12
10	5	400	0.1	3.5	0.625	5.59
100	2	400	0.1	3.5	0.781	2.41
100	2	400	0.5	3.5	6.25	2.68
50	2	400	0.5	3.5	6.25	2.24
35	2	400	0.5	3.5	8.75	1.93
35	2	800	0.2	3.5	2.19	4.29
100	2	800	0.2	3.5	3.13	5.35

In Figure 14 the crack spacings are presented so that the abscissa shows the minimum crack distance calculated by Equation 55. The ordinate shows the crack spacings from the present model. In addition, the best limits have been drawn with the second line having the slope twice that of the first line. The slopes of the lines are $8/3$ and $16/3$.

In Figure 15 the tensile strength of the composite is presented using the function of strength calculated by Equation 57. It is seen that there is a clear linear correlation. The slope of the regression line is about $3/8$.

The analysis shows that for composites with randomly oriented short fibres the following equations can be used.

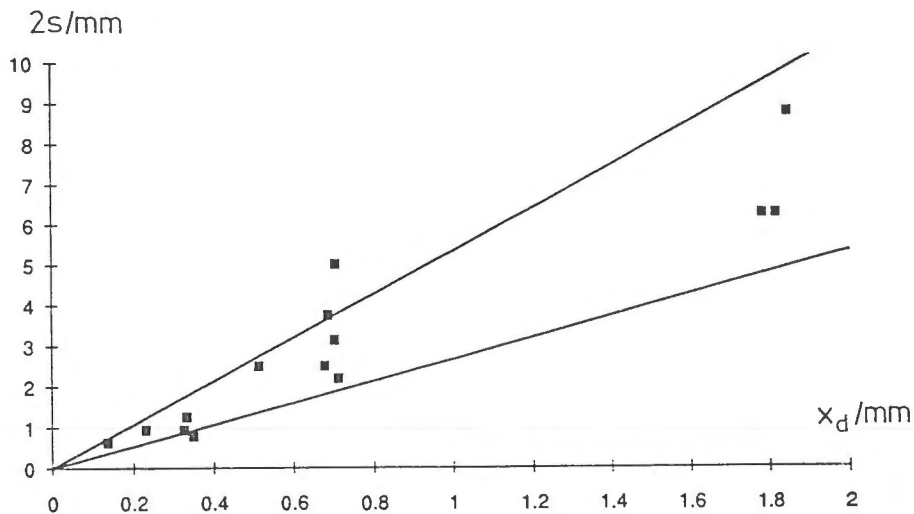


Figure 14. The relationship between the crack spacing of composites with randomly oriented short fibres according to the present model and the minimum crack spacing of composites with aligned short fibres according to the ACK model. The slopes of the lines presented are $8/3$ and $16/3$.

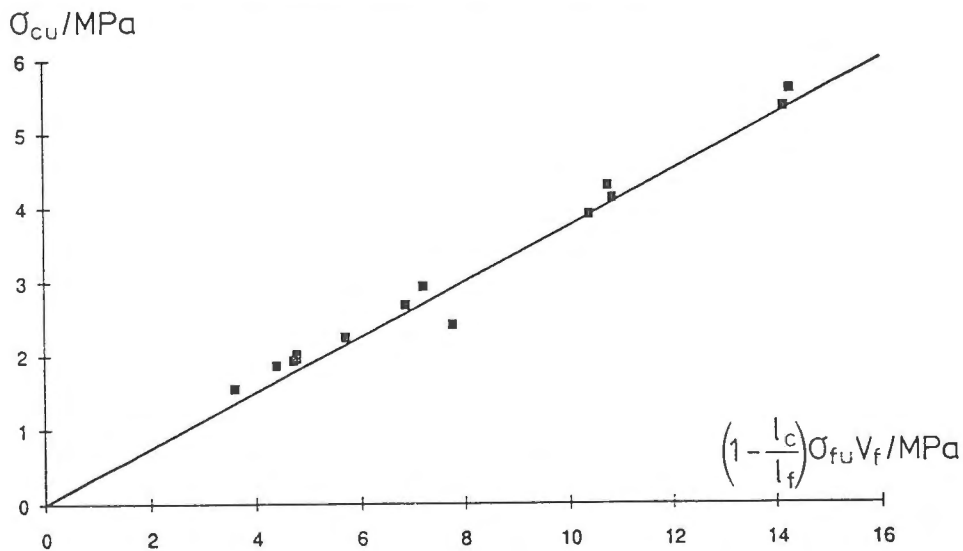


Figure 15. The relationship between the tensile strength of composites with randomly oriented short fibres according to the present model and the strength of composites with aligned short fibres according to the ACK model. The slope of the line presented is $8/3$.

$$x_d = \frac{8 l_f - \sqrt{l_f^2 - 4 l_f x}}{2} \quad (59)$$

and

$$\sigma_{cu} = \frac{3}{8} \left(1 - \frac{l_c}{l_f} \right) \sigma_{fu} V_f \quad (60)$$

CONCLUDING REMARKS

A statistical model of the tensile constitutive relation of fibre-reinforced concrete was established. The model takes into account both the single-fracture and multiple cracking. The model may also be applied to other brittle matrix composites, e.g. ceramics.

The modelling of the single-fracture mode is based on the fibre pull-out. The pull-out model used in this study is based on the model of Naaman & al. (1991). It includes the elastic and frictional shear stresses, the contribution of matrix deformation and the decaying of the frictional stress transfer.

The cracks are supposed to initiate when the matrix stress or strain reaches the critical values, σ_{mu} or ϵ_{mu} , respectively. However, according to Shah (1990) the cracking strength of the matrix increases with increasing fibre content. Therefore, a fracture mechanics approach to the criteria of cracking should be developed.

In multiple cracking, constant frictional stress transfer is assumed. The cases of stress transfer for different embedded lengths were introduced. It is assumed that every fibre has a so-called symmetry fibre that carries the load in the neighbouring crack. The average values are evaluated from effects of fibres with different orientations and embedded lengths.

In the single-fracture mode, the strain depends on the specimen length, unlike in the case of the multiple-cracking stage.

It was seen that in the multicracking stage the orientation efficiency factor for randomly oriented short fibres was not 1/2 as obtained by Equation 14. Instead, it was found to be 3/8.

The new proposed model can be used in designing and tailoring new FRC composites. In addition, it can be used in analyzing structures, e.g. beams.

ACKNOWLEDGEMENTS

This study is part of the research programme "Composite Materials and Structures in the Construction Industry" and was supported by the Technical Research Centre of Finland.

REFERENCES

Aveston, J., Mercer, R. A. & Sillwood, J. M. 1974. Fibre reinforced cements – scientific foundations for specifications. Composites – standards, testing and design. Conference Proceedings National Physical Laboratory. IPC Science and Technology Press, Guildford. S. 93–103.

Bentur, A. & Mindess, S. 1990. Fibre Reinforced Cementitious Composites. London. Elsevier Science Publishers Ltd. 449 s.

Naaman, A.E., Namur, G.G., Alwan, J.M. & Najm, H.S. 1991. Fiber Pullout and Bond Slip. I: Analytical Study. Journal of Structural Engineering, Vol 117, No. 9. ASCE. s. 2769–2790.

Shah, S. P. 1990. Toughening of Quasi-Brittle Materials due to Fibre Reinforcing. In: Shah, S. P. (edit.) Micromechanics of Failure of Quasi-Brittle Materials. London. Elsevier. pp. 1–11.

Wang, Y. 1985. Mechanics of Fibre Reinforced Concrete. MSc Thesis. Department of Mechanical Engineering, Massachusetts Institute of Technology. 175 s.

Wang, Y., Backer, S. & Li, V.C. 1989. A statistical tensile model of fibre reinforced cementitious composites. Composites, Vol 20, No 3. s. 265–274.

APPENDIX. THE EFFECT OF FIBRE ORIENTATION

The formulas derived earlier for multiple cracking are valid only for aligned fibres. When the fibre orientation is taken into account, the formulas change as follows. Let the fibres lie at the angle θ measured from the direction of the external load. Then the different load transferring cases are

1. If $l \leq l_x/2$, the fibre slips and $P = t_d l$, where t_d is the dynamic shear flow.

$$c = l_x/2 \quad (61)$$

$$h_1 = 0 \quad (62)$$

$$h_2 = 0 \quad (63)$$

2. If $l > l_x/2$

$$a = 2s/\cos\theta - \frac{1}{2}(l - l_x/2)$$

(a) If $a > l_x/2$, the fibre slips in the neighbouring crack. The force is totally transferred to the matrix (Figures 2, 3 and 4).

$$c = l_x/2 \quad (64)$$

$$h_1 = \min(2s/\cos\theta - c, l_x/2) \quad (65)$$

$$h_2 = \min(l - 2s/\cos\theta, l_x/2) \quad (66)$$

(b) If $2s/\cos\theta - l + l_x/2 < 0$, the fibre does not slip in the neighbouring crack. The forces of the fibre in both cracks are equal (Figures 5 and 6).

$$c = \min(s/\cos\theta, l_x/2) \quad (67)$$

$$h_1 = h_2 = c \quad (68)$$

(c) If $a \leq l_x/2$, the fibre slips in the neighbouring crack. The force is partially transferred to the matrix (Figure 7).

$$c = a \quad (69)$$

$$h_1 = h_2 = 2s/\cos\theta - c \quad (70)$$

The force transferred to the matrix between the cracks can be evaluated by examining the following cases.

1. $l \cos\theta > 2s$.

The fibre and its symmetry fibre are situated overlapping between the cracks.

$$h_2 \leq h_1.$$

$$T(x) = \begin{cases} 2t_f x, & 0 \leq x \leq h_2 \cos\theta \\ t_f(x + h_2 \cos\theta), & h_2 \cos\theta \leq x \leq h_1 \cos\theta \\ t_f(h_1 + h_2) \cos\theta, & h_1 \cos\theta \leq x \leq s \end{cases} \quad (71)$$

$$T(x=s) = \begin{cases} 2t_f s, & h_2 \cos\theta > s \\ t_f(s + h_2 \cos\theta), & h_1 \cos\theta > s \\ t_f(h_1 + h_2) \cos\theta, & h_1 \cos\theta < s \end{cases} \quad (72)$$

$$\overline{T(x)} = \begin{cases} t_f s, & h_2 \cos\theta > s \\ \frac{1}{s} t_f \cos\theta \left(\frac{1}{2 \cos\theta} s^2 - \frac{1}{2} h_2^2 \cos\theta + h_2 s \right), & h_1 \cos\theta > s \\ \frac{1}{s} t_f \cos\theta \left(-\frac{1}{2} h_1^2 \cos\theta - \frac{1}{2} h_2^2 \cos\theta + h_1 s + h_2 s \right), & h_1 \cos\theta < s \end{cases} \quad (73)$$

2. $l \cos \theta < s$ or $s > l_x \cos \theta/2$.

The fibre and its symmetry fibre or their normal forces are not situated overlapping between the cracks.

$$T(x) = \begin{cases} t_f x, & 0 \leq x \leq c \cos \theta \\ P \cos \theta, & c \cos \theta \leq x \leq s \end{cases} \quad (74)$$

$$T(x = s) = P \cos \theta \quad (75)$$

$$\overline{T(x)} = \frac{1}{s} \int_0^s T(x) dx = \frac{1}{s} \cos \theta \left[\frac{1}{2} t_f c^2 \cos \theta + P(s - c \cos \theta) \right] \quad (76)$$

3. $s < l_x \cos \theta/2$ and $s < l \cos \theta \leq 2s$.

The fibre and its symmetry fibre and their normal forces are situated partially overlapping between the cracks.

$$l_m = \min(2s / \cos \theta - l, l_x/2)$$

$$T(x) = \begin{cases} t_f x, & 0 \leq x \leq l_m \cos \theta \\ t_f l_m \cos \theta, & l_m \cos \theta \leq x \leq s \end{cases} \quad (77)$$

$$T(x = s) = t_f l_m \cos \theta \quad (78)$$

$$\overline{T(x)} = \frac{1}{s} t_f \cos \theta \left[\frac{1}{2} l_m^2 \cos \theta + l_m (s - l_m \cos \theta) \right] \quad (79)$$